Design and Simulation of Electro-fabricated MEMS Microhotplate for Gas Sensor Applications

2006 J. Phys.: Conf. Ser. 34 643

(http://iopscience.iop.org/1742-6596/34/1/106)

Institute of Physics Publishing Journal of Physics: Conference Series **34** (2006) 643–649
doi:10.1088/1742-6596/34/1/106 International MEMS Conference 2006

Design and Simulation of Electro-fabricated MEMS Micro-hotplate for Gas Sensor Applications

A. Wisitsoraat, A. Tuantranont, and T. Lomas

Nanoelectronics and MEMS Laboratory, National Electronics and Computer Technology Center (NECTEC), 112 Thailand Science Park, Phaholyothin Rd., Klong Luang, Pathumthani 12120 Thailand

Tel: +662-564-6900, Fax: +662-564-6771, Email: anurat.wisitsoraat@nectec.or.th

Abstract. In this paper, we present the simulation results of a new MEMS micro-hotplate design for gas sensor applications. The structure is designed to be fabricated on a glass substrate by the low cost process including physical vapor deposition, photolithography, electroplating, and photoresist-sacrificed process. The electro-thermo-mechanical behaviors of the proposed structure have been simulated by CoventorWareTM. In the simulation, the effects of thickness of the NiCr heater layer temperature, mechanical deflection, stress, and power consumption are evaluated. The 3D simulation on results show that the temperature, displacement, stress and current density are pronounced at the center of the beam as desired. At the nominal sensor temperature of ~400 °C, the power consumption and Mises stress are greatly reduced from 126 to 7 mW and 1280 to 472 MPa as the thickness decreases from 5 to 0.25 μm. In contrast, the compressive beam deflection is not monotonically increased as thickness increases and it is maximum at the thickness of ~0.5 μm. Therefore, the simulation results indicate that the proposed design with 0.25 μm-thick NiCr heater requires very low power consumption of 7 mW with low stress suitable and acceptable membrane deflection for gas sensor applications.

1. Introduction

Semiconductor gas sensors normally require high power consumption because of their elevated operating temperature. In modern applications including wireless sensor network and portable sensor, low power consumption is very essential. The high power consumption problem of these sensors can be greatly reduced by employing micro-hotplate MEMS structure because temperature can be locally confined in small area with minimal heat conduction. Low power MEMS microhotplate structures fabricated by various silicon micromachining processes have been demonstrated [1-6]. However, the cost of the MEMS fabrication is still much higher than that of conventional commercial sensors. This prohibits their use in low cost applications.

In this paper, we propose a new MEMS micro-hotplate structure fabricated by electrofabrication process for gas sensor applications and present the simulation results of the proposed structure to determine suitable thickness for low power consumption. The MEMS micro-hotplate has been designed and verified using the CoventorWare^{TM}, FEM simulation tool from Coventor Inc. This is a powerful finite element program, which can be used in MEMS analysis. In this simulation, the Electro-Thermal-Mechanic solver (EthermMech) module is used to simulate the temperature and displacement distribution of the MEMS microheater. This solver computes the electrical potential

field, thermal, and displacement distributions resulting from an applied voltage through a resistive heater. The advantages of the simulation are cost, time, and performance of the device to be fabricated.

2. MEMS Microhotplate Design and 3D Model

The proposed MEMS micro-hotplate as shown in Fig. 1 utilizes centrally indented, doubly supported beam heater on which isolation, interdigitated electrode, and sensing layers are placed. The concept of centrally indented design is to produce local heating region at the center of continuous beam where the sensor is located. In this design, the size of central beam, wide beam, and anchor are 10μm x 15μm, 30 μm x 25μm, and 30 μm x 15μm, respectively, while the transition length between central and wide beam is 15 μm. The heater, isolation, electrode, and sensing layers are NiCr (Ni 80%: Cr 20%), Si_3N_4, Au, metal oxide (SnO_2), respectively. The thickness of isolation, electrode, sensing, and air-gap layers, are designed to be 1 μm, 0.3 μm, and 0.3 μm, 5 μm, respectively. The structure is to be fabricated on a glass substrate by the electro-fabrication process, which is the combination of physical vapor deposition, photolithography, electroplating, and photoresist-sacrificed process. The cost of the electro-fabrication method and chosen materials are obviously much lower than that of standard silicon-based MEMS fabrication process.

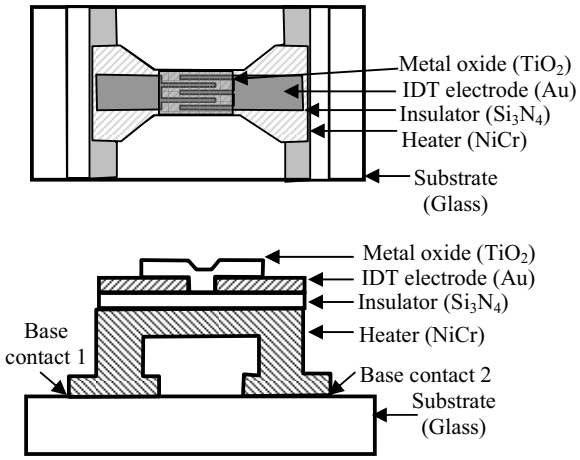

Fig. 1: The structure of the proposed MEMS micro-hotplate

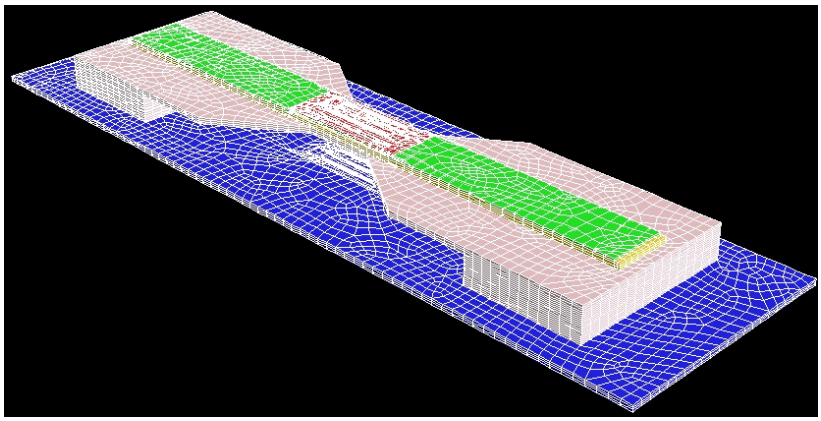

Fig. 2: 3D structure of MEMS microhotplate

CoventorWare™, commercially available finite element analysis software, is used to simulate the device to determine the relationship between applied voltage, temperature, mechanical deflection, stress, and power consumption. From the layout and defined processes, three-dimension model is generated as shown in Fig. 2. There are four layers in the simulation including NiCr, Si_3N_4, Au, and SnO_2 while the photoresist sacrificial layer is neglected. Material properties used in the simulation are listed in Table 1.

Table 1. Material properties of layers used in the MEMS micro-hotplate structure.

	NiCr	**Si_3N_4**	**Au**	**SnO_2**
Electrical conducivity (S/μm)	9.17e-1	1.0e-18	4.52e+1	2.1e-7
Thermal conductivity (J/Kg.K)	1.5e-5	1.9e-3	3.17e-4	9.8e-5
Thermal expansion coefficient (K^{-1})	1.6e-5	2.8e-6	1.42e-5	3.2e-6
Specific heat (W/μm.K)	4.6e+2	7.0e+2	2.28e+2	1.0.e+3
Density (kg/μm^3)	2.2e-15	3.1e-15	1.9e-14	7.0e-15
Young's Modulus (MPa)	2.2e+5	3.23e+5	7.72e+4	4.5e+4
Poisson's ratio	0.3	0.25	0.42	0.2

The extruded brick mesh is applied to the solid model. The whole structure is meshed with lateral element size of 10 μm and vertical element size between 1 and 0.25 μm depending on the thickness of NiCr layer. In the fine-structure region, which consists of Si_3N_4, Au, and SnO_2 layers, refined meshed is applied with element size of 0.3 μm. The 3D mesh structure is also demonstrated in Fig. 2. The combination of coarse and refined meshes is used in order to optimize the speed and quality of simulation.

3. Mathematical Formulation

The electrothermomechanical simulation is generally involved three sets of governing laws, Electrostatics, Heat transfer statics, and Mechanical statics.

For electrostatic simulation, the potential distribution, V, throughout the heater structure is determined by solving the Laplace's equation:

$$\delta \nabla^2 V = 0 \tag{1}$$

where δ is electrical conductivity of the heater material. The boundary condition for this equation is defined by the applied constant potential at both heater contacts, which are defined at the base contacts (surface 1 and 2 in Fig. 1) of the anchors of the beam and zero current in normal plane, J_n:

$$V_1 = V_s \text{ and } V_2 = 0,\ J_n = \delta \nabla V \bullet \overline{n} = 0 \tag{2}$$

where V_1 and V_2 are electric potential at base contact 1 and 2, respectively, V_s is the applied voltage to the microheater, and $\overline{n}$ is the normal unit vector. After the solution of potential is obtained, the electric field ($\overline{E}$), current density ($\overline{J}$), and Joule heating power (Q_e) are determined:

$$\overline{E} = -\nabla V, \quad \overline{J} = \delta \overline{E} \tag{3}$$

$$Q_e = J \cdot E = \delta |E|^2 \tag{4}$$

Next, the temperature distribution is calculated by inserting joule-heating power, Q_e, known from electrostatic simulation into the static heat transfer equation:

$$k \nabla^2 T + Q_e = 0 \tag{5}$$

The boundary condition of this equation is simply defined by fixing temperature at the base contacts to be room temperature ($T_1 = T_2 = T_0$ where T_1 and T_2, are temperature at base contact 1 and 2, respectively, T_0 = 300 K is room temperature). In this simulation, the heat convection boundary condition is neglected.

After temperature distribution is determined, the displacement and all other mechanical parameters are evaluated from the stress and mechanical static equation using the input thermal strain obtained from the solved temperature distribution and thermal expansion coefficient:

$$\sigma = E(\varepsilon - \varepsilon_T), \ \varepsilon_T = \alpha \Delta T \quad (6)$$

where σ, ε, ε_T , **E**, α, and ΔT are stress, strain, initial thermal strain, Young's Modulus matrix, thermal expansion coefficient, and differential temperature, respectively. The Young's Modulus matrix includes linear Young's modulus and Poisson's ratio. In finite element simulation, the mechanical static equation is transformed into a system of linear equation of displacement versus input force and the displacement vector is solved from the equilibrium matrix equations:

$$\begin{aligned} \frac{\partial \sigma_{xx}}{\partial x} + \frac{\partial \sigma_{xy}}{\partial y} + \frac{\partial \sigma_{xz}}{\partial z} + F_x = 0 \\ \frac{\partial \sigma_{yx}}{\partial x} + \frac{\partial \sigma_{yy}}{\partial y} + \frac{\partial \sigma_{yz}}{\partial z} + F_y = 0 \\ \frac{\partial \sigma_{zx}}{\partial x} + \frac{\partial \sigma_{zy}}{\partial y} + \frac{\partial \sigma_{zz}}{\partial z} + F_z = 0 \end{aligned} \quad (7)$$

where σ_{ij}, i,j ={x,y,z}, are stress elements and F_i are applied force per unit volume in x,y,z coordinate. The boundary condition of this equation is simply defined by anchoring at the base contacts to the substrate by setting zero displacement on the surface. The external applied force in all direction is also zero. All other mechanical parameters such as Mises stress can be determined from the known displacement distribution.

4. Simulation Results

The selected 3D simulation results of the structures with thin and thick heating layers are shown in Fig. 3 and 4 respectively. For a typical thin beam heating structure, it can be seen from Fig. 3 (a) that the beam begin to displace from the transition edges toward the center and the maximum displacement is ~1.0 μm. It should be noted that the displacement is mainly in z-direction but there are also x-y displacements occurred mostly near transition edges.

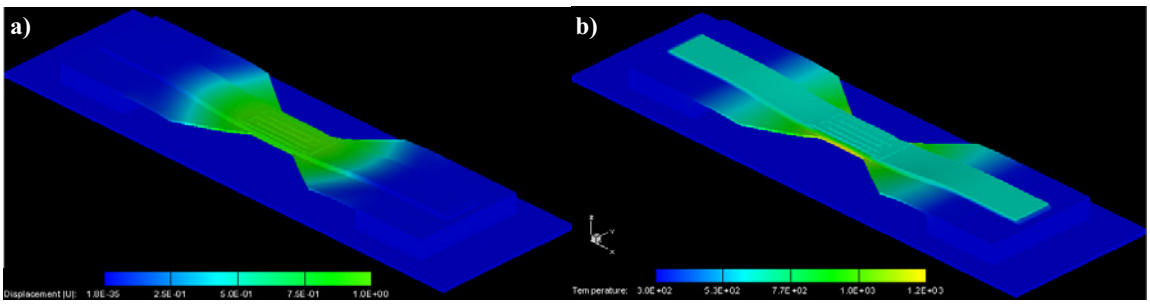

Fig. 3: 3D simulation of a) displacement and b) temperature distribution of the structure with 0.5 μm thick NiCr heater beam at 0.35 V applied voltage.

Similarly from Fig. 3 (b), the heater temperature increases from the transition region to reach the maximum value of ~1100 K at the center of NiCr heating layer. However, the temperature is uniformly distributed throughout interdigitated electrode and sensing layers and the temperature of the sensing layer is ~670 K, considerably lower than the maximum heater temperature. Thus, the 1.0 μm-thick Si_3N_4 isolation layer causes a significant temperature drop between the heater and sensor. This is undesirable effect but 1.0 μm-thick Si_3N_4 isolation layer is needed to ensure proper electrical isolation

at the operating temperature. It should be noted that displacement and temperature distribution for the structure with thicker heating layer are similar to this case except that x-y displacements near transition edges increases as the heating layer thickness increases.

For a typical thick beam heating structure, it can be seen from Fig. 4 (a) that the heater current density increases from the anchor edges to reach the maximum value of ~8×10^9 pA/μm^2 at the center of NiCr heating layer and there is no current in other layers as expected. The calculated Mises stress distribution, Fig. 4 (b), reveals that most of stress actually occurs in the interdigitated and sensing area. This result suggests that careful attention should be paid to prevent possible fracture failure of the sensing layer due to the local stress.

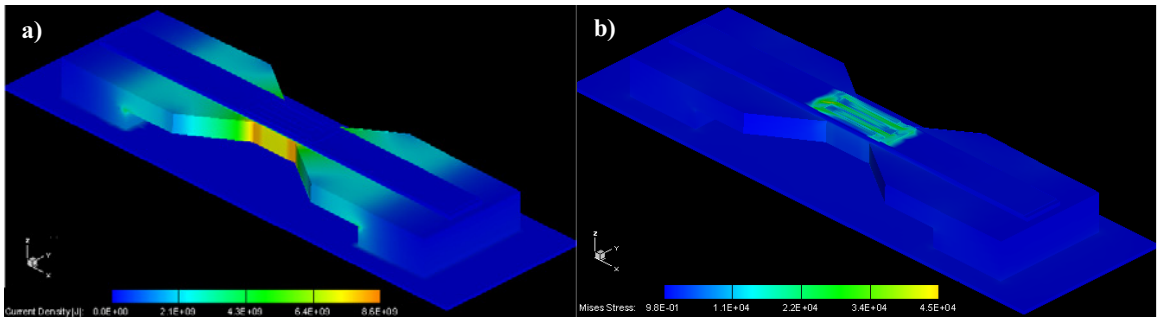

Fig. 4: 3D simulation of current density and stress distribution of the structure with 5 μm thick NiCr heater beam at 0.35 V applied voltage

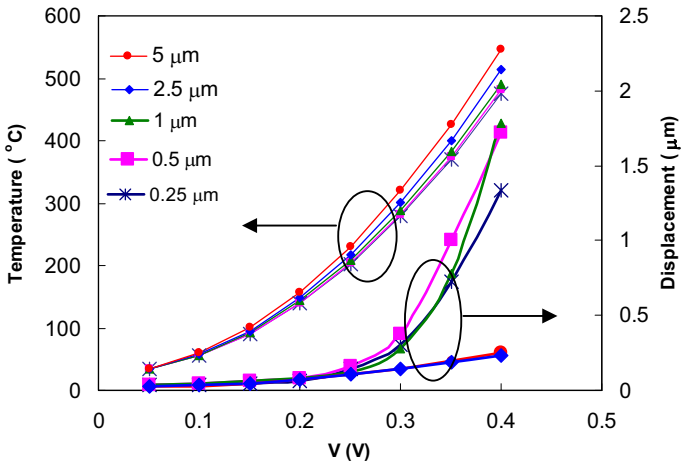

Fig. 5: Sensor temperature and maximum deflection vs. applied voltage for different NiCr beam thickness

The sensor temperature and maximum displacement plots vs. applied voltage for different NiCr beam thickness are shown in Fig. 5. It can be seen that the temperature increases nonlinearly as a function of applied voltage for all cases. It is found that this nonlinear function may be estimated by a power law. In contrary, the displacement tends to increase exponentially with applied voltage. It should be noted that for thick beam heater, the exponential regime would clearly occur at a higher applied voltage.

The average Mises stress and total power consumption plots vs. applied voltage for different NiCr beam thickness are illustrated in Fig. 6. It can be seen that the average Mises stress also increases nonlinearly as a function of applied voltage for all cases. It is found that this nonlinear function may

also be estimated by a power law. Similarly, the power consumption increase quadratically as function of applied voltage.

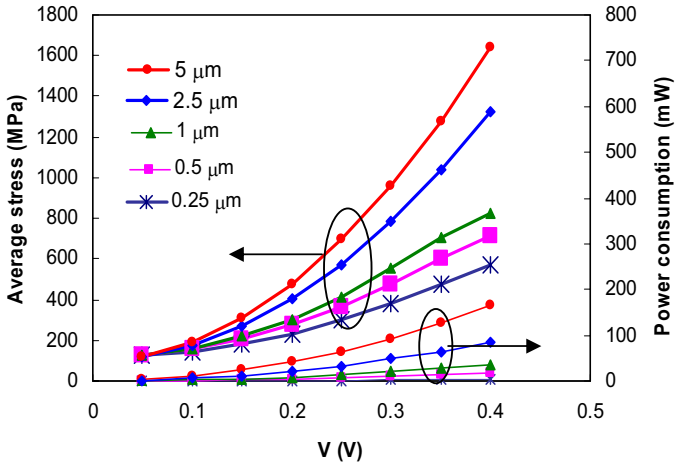

Fig. 6: Power consumption and thermal stress vs. applied voltage for different NiCr beam thickness

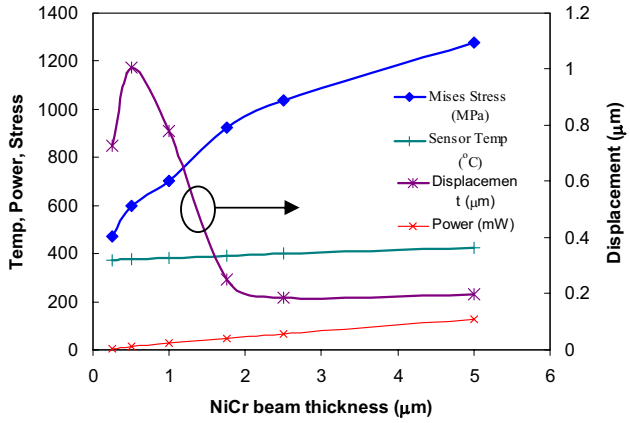

Fig. 7: Temperature, displacement, power consumption, and Mises stress vs. NiCr beam thickness at 0.35 V operating voltage.

The overall MEMS heater characteristics as a function NiCr heating layer thickness at the nominal sensor operating temperature of ~400 °C are summarized in Fig. 7. It can be seen that the compressive beam deflection is maximum at the thickness of ~0.5 μm and become insensitive to the thickness above ~2 μm. In contrast, the power consumption and Mises stress are greatly reduced from 126 to 7 mW and 1280 to 472 MPa as the thickness decreases from 5 to 0.25 μm. From the simulation results, it can be primarily decided that the design with 0.25 μm-thick NiCr heater should be an optimum choice for gas sensor applications because it consumes very low power consumption of 7 mW. In addition, it has the lowest average Mises stress of 500 MPa and acceptable maximum displacement of ~0.8 μm. It should be noted that the minimum thickness of NiCr heater is determined to 0.25 μm based on structural rigidity and practicality of pinhole free thin film fabrication.

5. Conclusion

In conclusion, a new MEMS microheater with centrally indented beam design has been simulated for gas sensor applications. In the simulation, the effects of thickness of the NiCr heater layer temperature, mechanical deflection, stress, and power consumption are evaluated. The simulation results show that the temperature, displacement, stress and current density are pronounced at the center of the beam as desired. In addition, the sensor operating temperature in the range of 300-450°C is achieved with low applied voltage of 0.3-0.4 V. At a sensor operating temperature, the power consumption and Mises stress are found to greatly reduced as the thickness decreases. In contrast, the compressive beam deflection is maximum at a particular thickness of ~0.5 μm. The simulation results suggest that the proposed design with 0.25 μm-thick NiCr heater layer should be the optimal parameter because it requires very low power consumption of 7 mW with low stress suitable and acceptable membrane deflection suitable for gas sensor applications. This work is a preliminary study for design optimization of low-cost non-silicon based MEMS gas sensors.

References

[1] R. Cavicchi, et al., "Growth of SnO_2 films on micromachined hotplates", Appl. Phys. Lett. 66, 1995, 812-4.

[2] S. Semancik, et al., "Microhotplate platforms for chemical sensor research" Sens Act. B77, 2001, 579–91.

[3] R. Cavicchi, J. Suehle, K. Kreider, M. Gaitan, "Fast temperature programmed sensing for microhotplate gas sensors", IEEE Electron Devices Letters, Vol. 16, No.6, pp.286-288, June 1995.

[4] F. Dimeo Jr., S. Semancik, R. Cavicchi, J. Suehle, N. Tea, M. Vaudin, J. Kelliher, "Silicon microhotplate arrays as a platform for efficient gas sensing thin film research", Mater. Res. Soc. Symp. Proc. Vol. 444, p. 203, 1997.

[5] Semancik S.,Cavicchi R.,Wheeler M.,Tiany J., Poirier G.,Walton,"R. Microhotplate platforms for chemical sensor research" Sens. Actuators. B77 2001, 77, pp. 579–91.

[6] M. Afridi, A.Hefner, D.Berning, C. Ellenwood, A.Varma, B.Jacob, and S. Semancik "MEMS-based embedded sensor virtual components for system-on-a-chip (SoC)", Solid-State Electronics Vol. 48, pp. 1777-1781, 2004.